# THE SHIFTING SHAPES OF FRICTIONAL FLUIDS

## LAS FORMAS CAMBIANTES DE LOS FLUIDOS CON FRICCIÓN

B. Sandnes[a †], E. G. Flekkøy[b], K. J. Måløy[b] and J. A. Eriksen[b]

a) Multidisciplinary Nanotechnology Centre, College of Engineering, Swansea University, Singleton Park, Swansea SA2 8PP, UK, b.sandnes@swansea.ac.uk†
b) Department of Physics, University of Oslo, Sem Sælandsvei 24, PO Box 1048 Blindern, 0316 Oslo, Norway
† corresponding author

Remarkable shapes and patterns appear in multiphase flow experiments with frictional fluids. Here we explore the rich dynamics, and map the emerging morphologies in a phase diagram.

Se observan interesantes formas y patrones en experimentos multifásicos sobre fluídos con fricción. Aquí, exploramos esa rica dinámica, y "mapeamos" las morfologías emergentes en un diagrama de fases.

**PACS:** Pattern formation in granular systems, 45.70.Qj; multiphase flows, 47.55.-t; compaction granular solids, 45.70.Cc; general flow instabilities, 47.20.-k

## INTRODUCTION

While displacement patterning in dry granular materials [1,2] and density matched granular suspensions [3-5] have been studied before, the world of settling granular mixtures, where inter-particle friction plays a dominant role, remains largely unexplored. Here we focus on pattern formation in such a frictional fluid, and find a surprising diversity in the morphologies that emerge. Based on our experimental and theoretical results [6-8] we draft a crude phase diagram of the different pattern formation modes we encounter and the phase boundaries between them.

## EXPERIMENT

The experiment is simple: Air contained in a syringe is injected into a generic granular-liquid mixture confined in a 500 $\mu m$ gap between two parallel glass plates of a Hele-Shaw cell (Fig. 1). The syringe pump is driven at a constant compression rate $q$, and the volume of compressible air in the syringe, $V_{air}$, adds an adjustable compliance (or stiffness) to the system. The initial filling fraction of granular material –glass beads of 100 $\mu m$ average diameter– is denoted $\varphi$, where we normalize by the close-packing fraction, i.e. $\varphi = 1$ for consolidated grains. The invading air/fluid interface displaces the mixture, and the shifting balance between the contending forces (pressure, frictional, viscous and capillary forces) determines the dynamics as we explore the full range of the chosen experimental variables. In the following we give a somewhat brief description of the most characteristic morphologies that we observe, and refer to a recent paper [8] for more detail regarding experimental setup, results and theoretical considerations.

## FRICTIONAL REGIME

*Frictional fingers.* At low compression rate ($0.01 < q < 0.1$ *ml*/*min*) the invading interface moves slowly and bulldozes up granular material until a layer forms that jams in the gap of the cell. The interface becomes unstable, and fingers of air develop that spawn side-branches as they grow, creating a random labyrinthine structure [6,7]. Fig. 2 (a) shows an example of these frictional fingers, where the dense granular front is seen as a dark band along the interface.

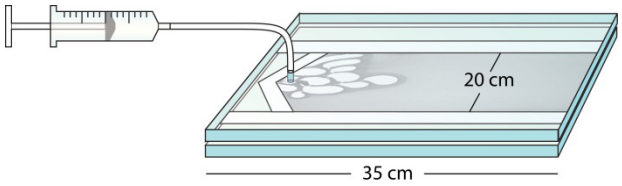


Figure 1: Air is injected into a granular-liquid mixture confined in the gap of a Hele-Shaw cell.

The gas pressure is balanced by the surface tension of the interface and the opposing frictional stress. These forces act locally, and the fingers develop a characteristic width that is independent of system size (unlike viscous fingers). Surface tension acts to widen the curved finger tip, while friction opposes wide fingers since they accumulate thick granular fronts. The characteristic width represents a balance between these two opposing influences. If we increase the amount of granular material in the system, the increased friction shifts the balance, resulting in narrower fingers.

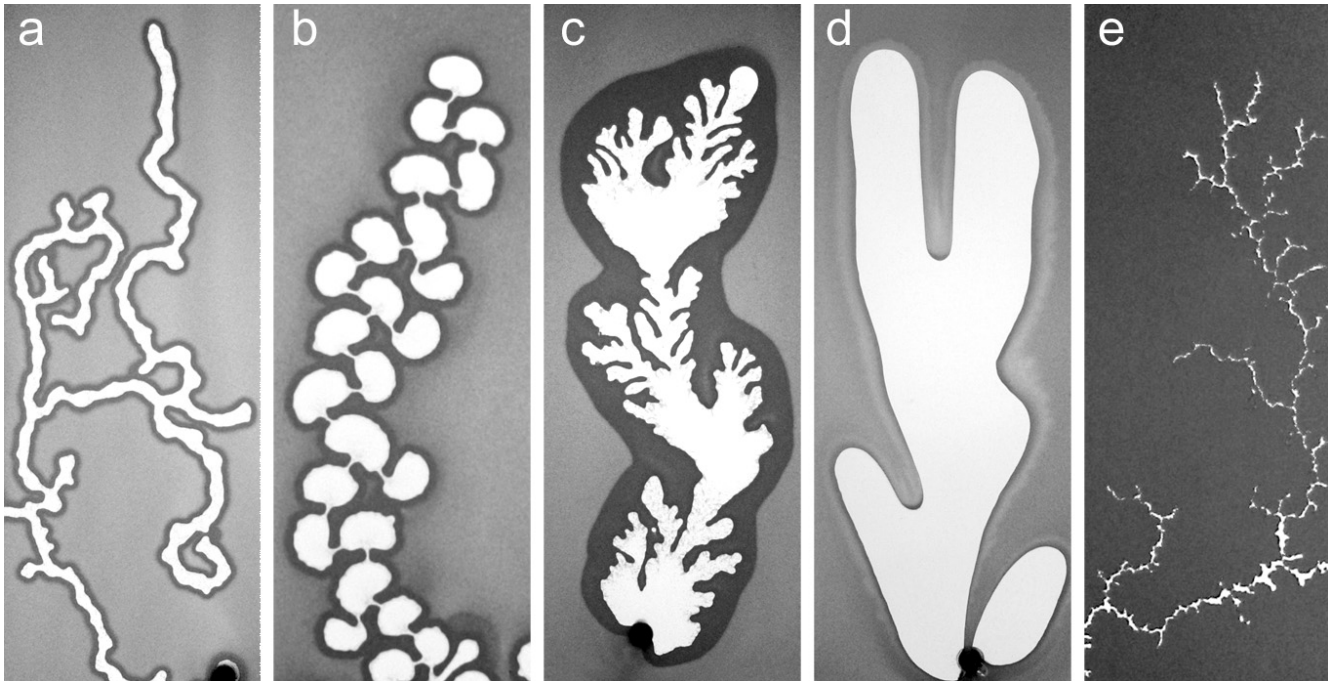


Figure 2: Shapes of air in frictional fluids. (a) frictional fingers (low rate, low packing fraction, high stiffness), (b) stick slip bubbles (low rate, intermediate solid fraction, low stiffness), (c) fluidized front "corals" (intermediate rate), (d) viscous fingers (high injection rate) and (e) fractures (high packing fraction).

*Stick slip bubbles.* Fig. 2 (b) shows a string of bubbles that have appeared in a stick slip fashion, one by one, at approximately 10 minutes intervals. The pump rate is the same as for the frictional fingers, but by either increasing the packing fraction or by increasing the compliance of the system (or both), the dynamics changes abruptly to this new dynamic mode. Each bubble scoops up a thick granular front, and breaking through this front requires a high gas pressure. In the stationary period, the constant driving of the pump compresses the gas and the pressure slowly builds until the jammed granular front finally yields. The interface yields at its weakest point, from which a narrow channel breaks through the jammed packing. The compressed gas expands, and a bubble inflates in the granular-liquid mixture.

VISCOUS REGIME

*Fluidized front (corals).* At flow rates greater than roughly 0.1 *ml*/*min*, the motion of the front is fast enough that fluid forces inside the packing overcome friction and prevent jamming of the front. The active front is continuously fluidized by the moving interface, and we are in a domain where viscous forces dominate the dynamics. Fig. 2 (c) shows a peculiar looking "coral" structure that grows at intermediate flow rates. The pattern develops in a two-stage process: first a bubble expands. Then narrow fingers start to invade the fluidized front surrounding the bubble. The less viscous gas penetrates the (more viscous) fluidized mixture driven by the pressure gradient across the front in a process of local viscous fingering. When one finger gets ahead of the rest, it accelerates, evolving into another bubble.

*Viscous fingers.* Cranking up the pump rate above 10 *ml*/*min* results in another transition in the system: As Fig. 2 (d) shows, there is no longer a dark front of accumulated granular material surrounding the interface. The granular material is re-suspended by the flow, and we are now effectively dealing with a granular suspension. The Saffman-Taylor instability [9] in granular suspensions has been studied by other authors [3,4], and like Chevalier *et al.* [3], we find an early destabilization and branching of the viscous fingers due to the noise associated with the granularity of the suspension (Fig. 2 (d)).

SOLID REGIME

*Fractures.* What happens when we increase the packing fraction considerably? At $\varphi \sim 0.9$ the granular material fills the gap in the cell, but is not fully compacted into a close packed configuration. The material is a solid, yet deformable (porous) medium. Fig. 2 (e) shows that injection of gas into this system results in fractures. The fractures are several particle diameters wide, and the morphology is fractal of appearance. The fractures grow intermittently, in a stick slip fashion similar to the bubbles in Fig. 2 (b).

*Porous media.* If the packing fraction is increased further, the system ultimately reaches the close packing limit ($\varphi = 1$), and is effectively a consolidated porous medium. The displacement of fluid occurs in the pore space network defined by the rigid granular matrix. Local fluctuations in the threshold capillary pressures of pores, in addition to the viscous pressure gradient in the cell, determine the displacement dynamics [9-12]. There are two main pattern formation modes: Capillary fingering at low rates, where viscous forces are negligible and pores are invaded in sequence depending on their threshold capillary pressure, and viscous fingering at high rates, where

the displacement dynamics is governed by the pressure field in the cell. Capillary fingering progresses from pore to pore in random directions, forming compact structures in an invasion percolation process. Viscous fingers in porous media on the other hand follow the pressure gradient in the cell generated by the displacement of the fluid. They grow in thin branching fingers towards the edge of the cell in fractal structures that look similar to those obtained in diffusion limited aggregation (DLA) processes.

## PHASE DIAGRAM

Summarizing the results, Fig. 3 shows a qualitative phase diagram of the morphologies as a function of compression rate ($q$) and the inverse of the packing fraction ($\varphi^{-1}$), i.e. from high to low packing fraction. Both axes are log-scale, and the phase borders are intended as "guides to the eye" only.

The medium changes character from porous medium to deformable solid to frictional fluid as the packing fraction decreases. Each of these regimes have characteristic morphologies associated with them, and at low rate these are capillary fingering (porous media), fractures (deformable media) and frictional bubbles and fingers (frictional fluids) respectively.

The fluid dynamics of granular mixtures changes character from frictional to viscous flows (fluidized front, viscous fingering) as the rate is increased, and the two-phase flow in porous media undergoes a transition from capillary to viscous fingering for increasing rate. The fracture mode seems reasonably rate-independent within the limited parameter range studied here.

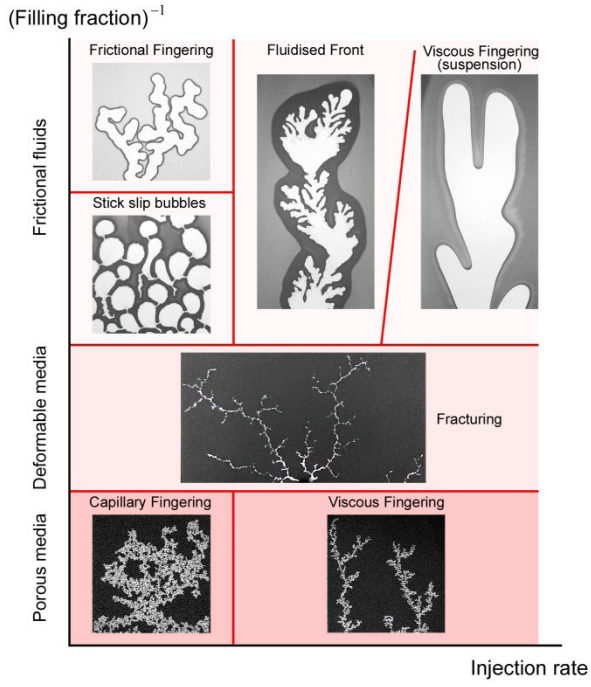


Figure 3: Phase diagram of pattern formation modes obtained by varying the packing fraction and compression rate over several orders of magnitude.

## HYDROPHOBIC GRAINS

So far we have considered displacement of a granular fluid mixture by a gas. While the pattern formation is to a large degree governed by the specifics of the system, it is interesting to speculate whether the mechanisms are of a more general nature. Figure 4 shows the result of an "inverted" experiment: A layer of dry hydrophobic grains (0.1 – 0.4 *mm* diameter) is confined in a Hele-Shaw cell (gap ~ 0.6 *mm*). As water is slowly injected into the cell, the dry hydrophobic material is pushed aside by invading water fingers (seen in black in the figure). The resulting patterns and the dynamics are similar to the frictional fingering process depicted in Figure 2 (a) as it is controlled by the capillary forces at the interface, and the frictional interactions in the granular material. The specific nature of these interactions are however expected to be different (dry vs. lubricated grains, incompressibility of the invading phase etc.), and will be investigated in future work.

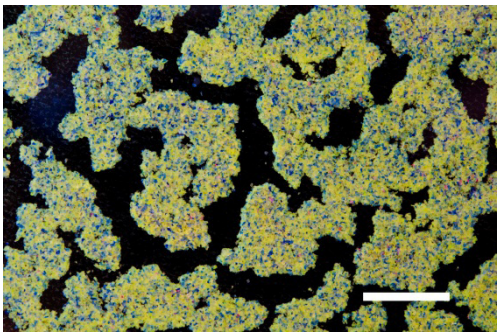

Figure 4: Fingers of water (black) penetrating dry hydrophobic granular material. Scale bar: 1 *cm*.

## CONCLUSIONS

We find that the fluid dynamics of granular mixtures is highly complex indeed. Interactions between pressure, frictional, viscous and capillary forces conspire to produce an ever changing landscape of shapes and patterns as the experimental conditions change. Here we have presented characteristic morphologies that emerge as a result of displacement by a gas, and we have outlined the physical mechanisms at play. By mapping the displacement dynamics onto a phase diagram, we provide a means of predicting the type of dynamics occurring for a given set of conditions.

## ACKNOWLEDGEMENTS

Dedicated to Henning A. Knudsen and Howard See.

[1] X. Cheng, L. Xu, A. Patterson, H. M. Jaeger and S. R. Nagel, Nat. Phys. **4**, 234 (2008).
[2] Ø. Johnsen, R. Toussaint, K. J. Måløy and E. G. Flekkøy, Phys. Rev. E **74**, 011301 (2006).
[3] C. Chevalier, A. Lindner and E. Clement, Phys. Rev. Lett. **99**, 174501 (2007).

[4] C. Chevalier, A. Lindner, M. Leroux, and E. J. Clement, Non-Newton. Fluid Mech. **158**, 63 (2009).
[5] Ø. Johnsen, C. Chevalier, A. Lindner, R. Toussaint, E. Clément, K. J. Måløy, E. G. Flekkøy and J. Schmittbuhl. Phys. Rev. E **78**, 051302 (2008).
[6] B. Sandnes, H. A. Knudsen, K. J. Måløy and E. G. Flekkøy, Phys. Rev. Lett. **99**, 038001 (2007).
[7] H. A. Knudsen, B. Sandnes, E. G. Flekkøy, and K. J. Måløy, Phys. Rev. E **77**, 021301 (2008).
[8] B. Sandnes, E. G. Flekkøy, H. A. Knudsen, K. J. Måløy and H. See, Nat. Commun. **2**, 288 (2011).
[9] P. G. Saffman and G. Taylor, Proc. R. Soc. London, Ser. A **245**, 312 (1958).
[10] K. J. Måløy, J. Feder and T. Jøssang, Phys. Rev. Lett. **55**, 2688 (1985).
[11] G. Løvoll, Y. Meheust, R. Toussaint, J. Schmittbuhl and K. J. Måløy, Phys. Rev. E **70**, 026301 (2004).
[12] R. Lenormand, Physica A **140**, 114 (1986).